Electronic Supplementary Material (ESI) for Catalysis Science & Technology.
This journal is © The Royal Society of Chemistry 2020

Supporting Information

Cooperative acid-base bifunctional ordered porous solids in sequential multi-step reactions: MOF *vs.* mesoporous silica

Francisco G. Cirujano*, Nuria Martín, Guangxia Fu, Chunmei Jia and Dirk De Vos*

KU Leuven, Celestijnenlaan 200F, 3001 Leuven, Belgium

1. Characterisation of the hybrid solids

Table S1. Composition and textural properties for amine-functionalized ordered mesoporous MCM-41 silica and Lys/MOF-808.

Catalyst	Si/Al	Surface area BET (m^2/g)	Average pore diameter (nm)[a]	N loading (mmol/g)[b]	Acidity (mmol/g)[c]
MOF-808	-	698	1.8	-	-
Lys/MOF-808		636	0.8	2.2	0.3
$MCM\text{-}41_A$	4000	743	3.9	-	-
$APMS/MCM\text{-}41_A$		508	2.1	1.8	0.0
$MCM\text{-}41_B$	59	973	2.9	-	-
$APMS/AlMCM\text{-}41_B$		685	2.3	1.7	0.6
$5APMS/AlMCM\text{-}41_B$		553	1.9	2.3	
$MCM\text{-}41_C$	28	845	2.9	-	-
$APMS/AlMCM\text{-}41_C$		642	2.3	1.6	-
$5APMS/AlMCM\text{-}41_C$		269	1.9	2.5	-
$MCM\text{-}41_D$	16	616	3.6	-	-
$APMS/AlMCM\text{-}41_D$		372	2.6	1.5	0.7
$5APMS/AlMCM\text{-}41_D$		145	2.7	2.2	-

[a]Obtained from the pore size distribution of the N_2 gas adsorption isotherms (see Fig. S1 right). [b]Obtained from combustion analysis. [c]Obtained from NH_3-TPD.

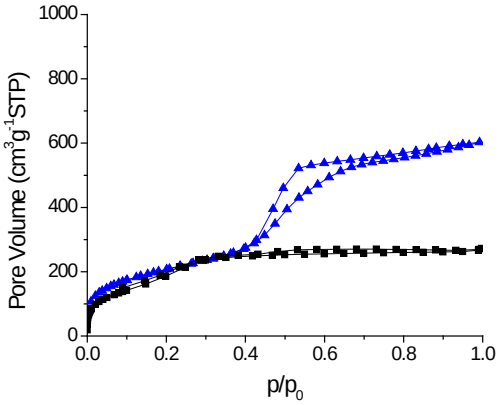
Pore Volume (cm3g-1STP)
p/p0

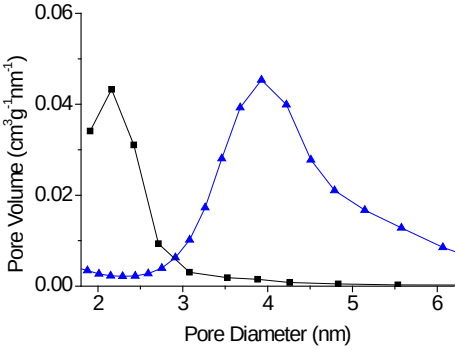
Pore Volume (cm3g-1nm-1)
Pore Diameter (nm)

(a)

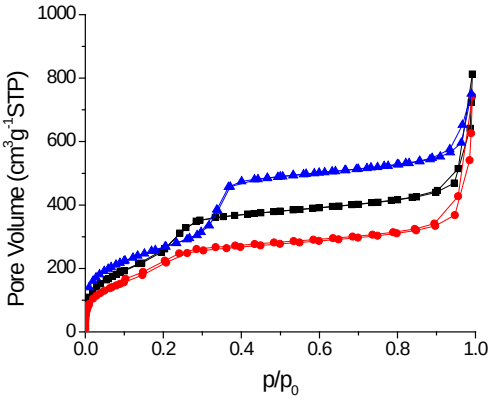
Pore Volume (cm3g-1STP)
p/p0

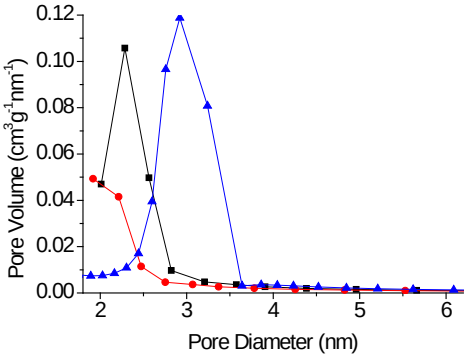
Pore Volume (cm3g-1nm-1)
Pore Diameter (nm)

(b)

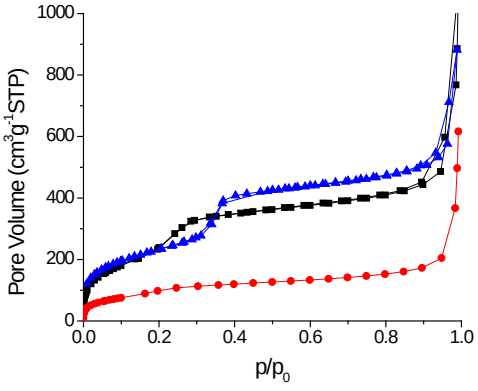
Pore Volume (cm3g-1STP)
p/p0

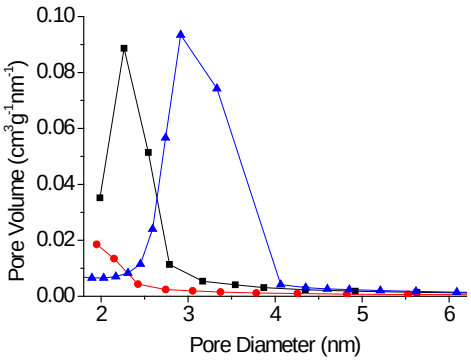
Pore Volume (cm3g-1nm-1)
Pore Diameter (nm)

(c)

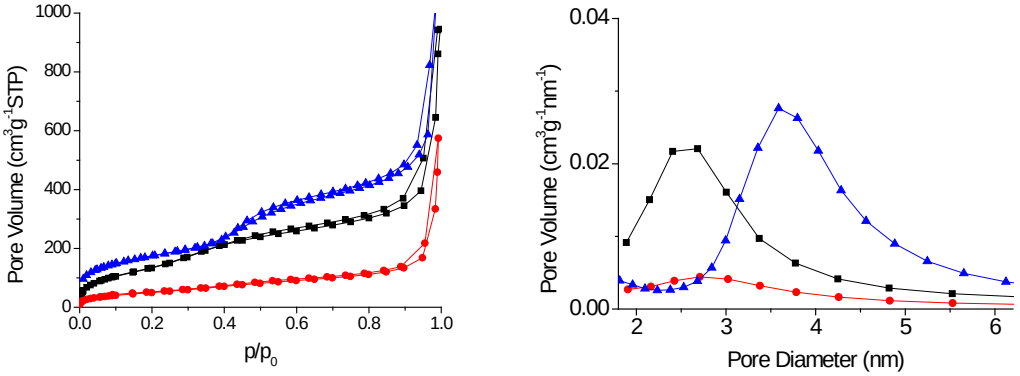

(d)

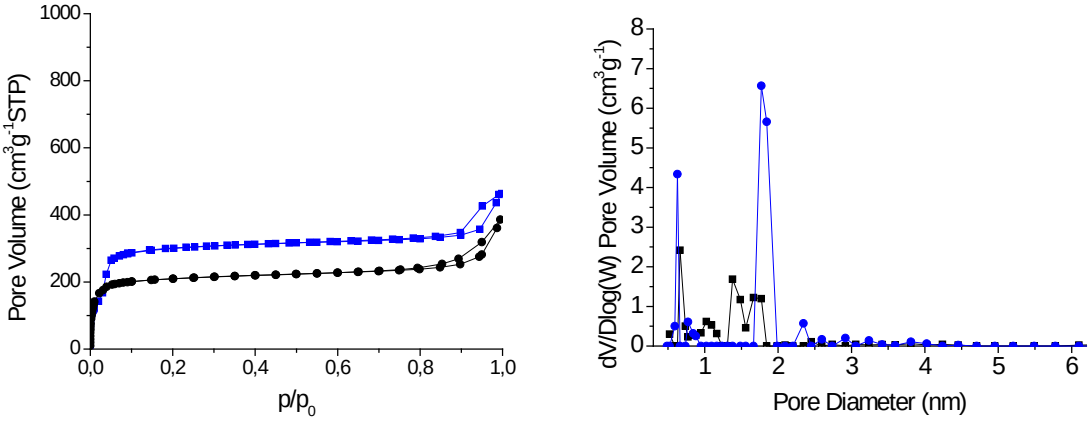

(e)

Figure S1. N_2 physisorption isotherms (left) and pore size distribution (right) of (a) MCM-41, (b) AlMCM-41 (Si/Al = 60), (c) AlMCM-41 (Si/Al = 30), (d) AlMCM-41 (Si/Al = 15), (e) MOF-80. AlMCM-41 or MOF-808 (blue curve), APMS/AlMCM-41 or Lys/MOF-808 (black curve), 5APMS/AlMCM-41 (red curve).

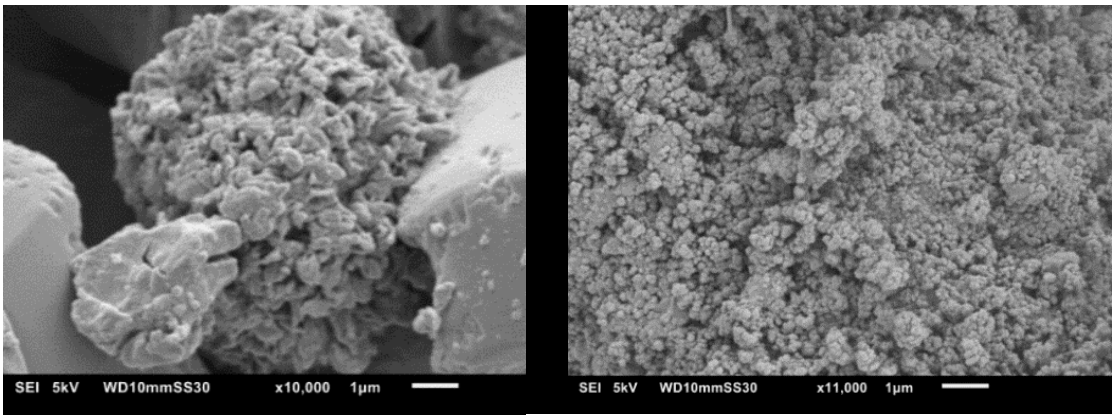

(a) (b)

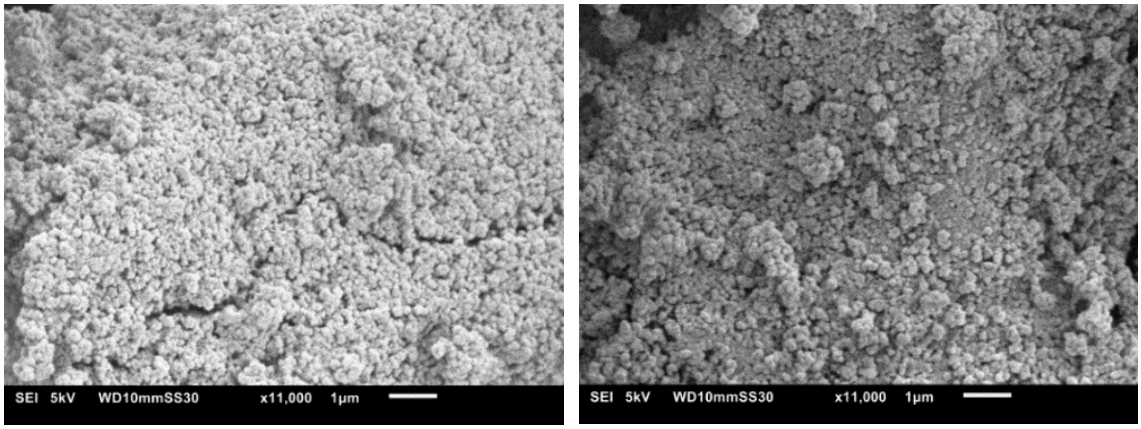

(c) (d)

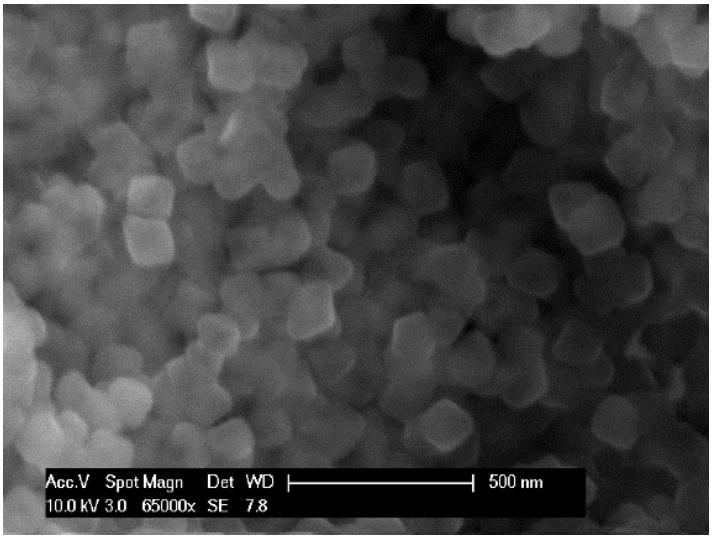

(e)

Figure S2. SEM images of (a) APMS/MCM-41$_A$, (b) APMS/AlMCM-41$_B$ (Si/Al = 60), (c) APMS/AlMCM-41$_C$ (Si/Al = 30), (d) APMS/AlMCM-41$_D$ (Si/Al = 15), (e) Lys/MOF-808.

2. Kinetic analysis

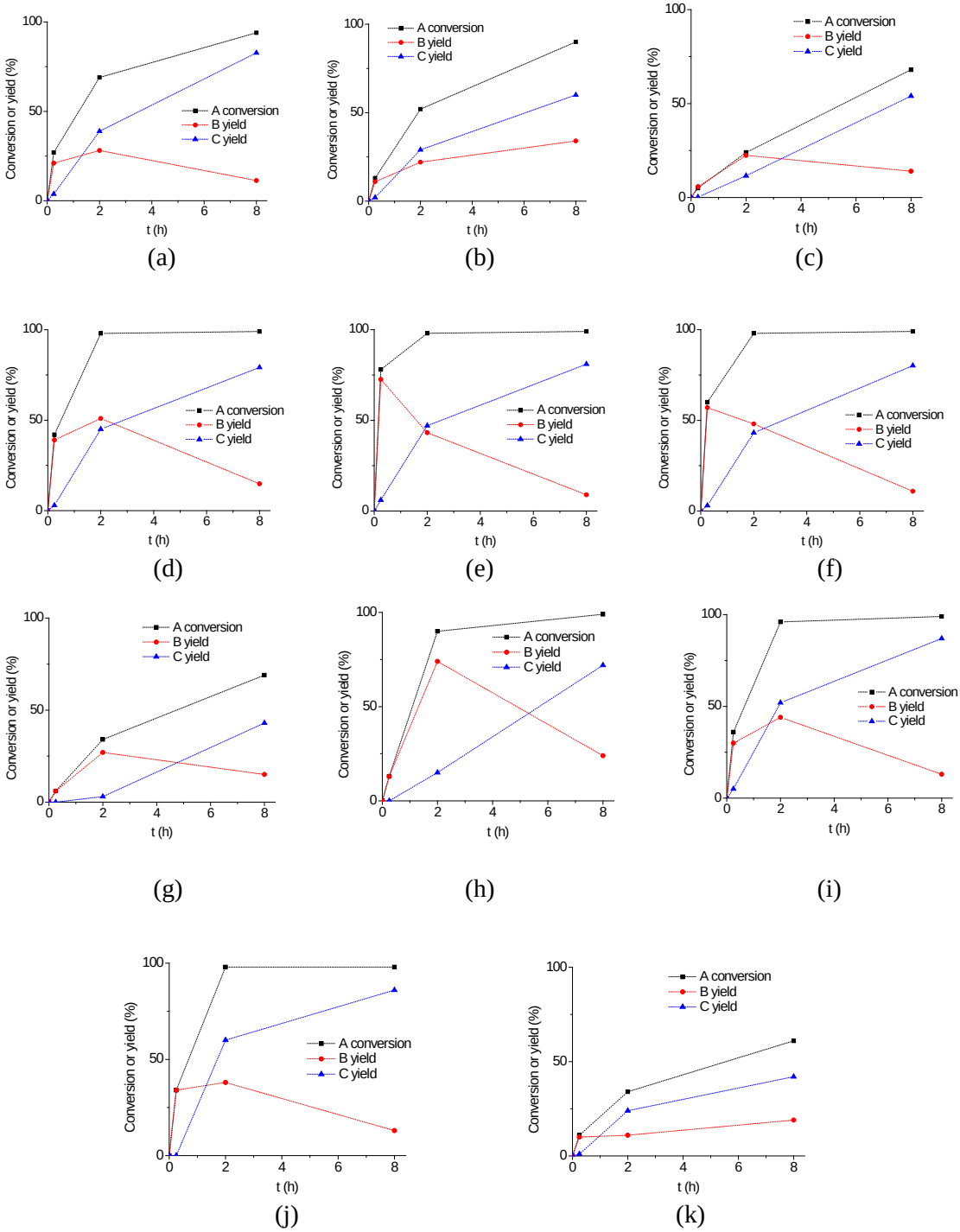

Figure S3 Kinetic plots for the conversion of benzaldehyde (A) into nitrostyrene (B) and alkylated indole (C) using AMPS/MCM-41$_A$ (a), AMPS/MCM-41$_B$ (b), AMPS/MCM-41$_C$ (c), Lys/MOF-808 (d), Lys/MOF-101 (e), Lys/UiO-66 (f), Lys (g), APMS, (h) Lys/MCM-41$_D$(i), Lys/MCM-41$_A$ (j) and Lys/MCM-41$_A$ (k) as catalysts.

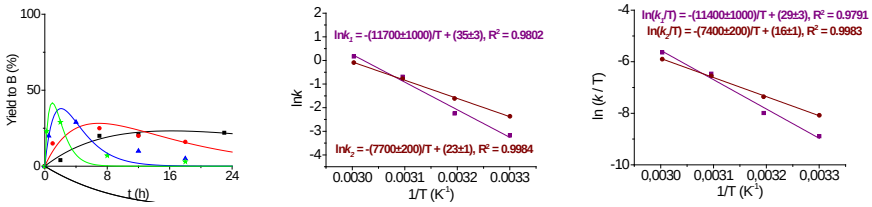

(a)

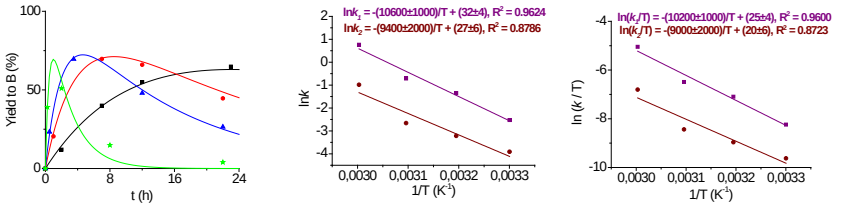

(b)

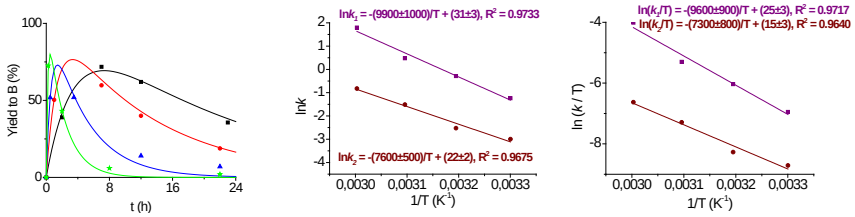

(c)

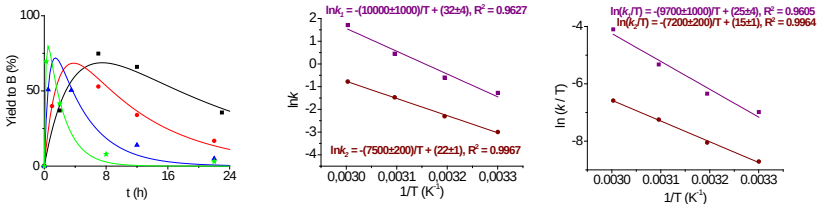

(d)

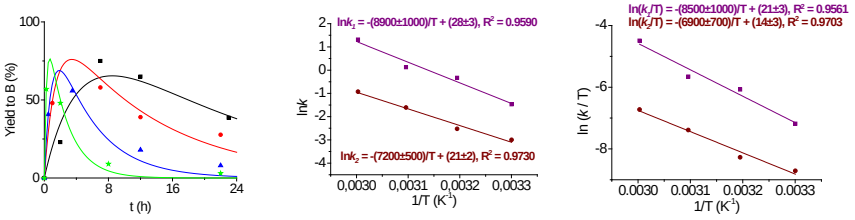

(e)

Figure S4. One-pot two-step nitro aldol- alkylation synthesis of substituted indole using: (a) Lys/MOF-808, (b) APMS/MCM-41, (c) APMS/AlMCM-41 (Si/Al = 60), (d) APMS/AlMCM-41 (Si/Al = 30), (e) APMS/AlMCM-41 (Si/Al = 15). On the left part, the fitting to the kinetic model is shown at 30 ºC (black curve), 40 ºC (red curve), 50 ºC (blue curve) and 60 ºC (green curve). On the right part, the Arrhenius, ln(*k*) *vs.* 1/T, and Eyring, ln(*k*/T) *vs.* 1/T, fitting is shown together with the standard error.

Table S2. Kinetic analysis of the one-pot two-step processes for different catalytic systems.

	T/ °C	k_1/ h^{-1}	E_1 (kJ/ mol)[a]	$\Delta^{\neq}H_1$ (kJ/ mol)[b]	A_1 (s^{-1})[a]	$\Delta^{\neq}S_1$ (J/mol ·K)[b]	k_2/ h^{-1}	E_2 (kJ/ mol)[a]	$\Delta^{\neq}H_2$ (kJ/ mol)[b]	A_2 (s^{-1})[a]	$\Delta^{\neq}S_2$ (J/mol ·K)[b]
Lys/ MOF-808	30	0.04	97	94	$4.4\cdot10^{11}$	35	0.09	64	62	$2.7\cdot10^{6}$	-64
	40	0.11					0.20				
	50	0.50					0.46				
	60	1.18					0.91				
APMS/ MCM-41_A	30	0.08	88	85	$2.2\cdot10^{11}$	10	0.02	78	75	$1.5\cdot10^{9}$	-31
	40	0.26					0.04				
	50	0.49					0.07				
	60	2.14					0.37				
APMS/ MCM-41_B	30	0.29	83	80	$8.1\cdot10^{10}$	10	0.05	63	61	$1.0\cdot10^{7}$	-73
	40	0.75					0.08				
	50	1.61					0.22				
	60	6.02					0.44				
APMS/ MCM-41_C	30	0.28	83	81	$2.2\cdot10^{11}$	10	0.05	63	60	$1.0\cdot10^{7}$	-73
	40	0.55					0.10				
	50	1.57					0.23				
	60	5.51					0.46				
APMS/ MCM-41_D	30	0.23	74	71	$4.0\cdot10^{9}$	-22	0.05	60	57	$3.7\cdot10^{6}$	-81
	40	0.72					0.08				
	50	1.13					0.20				
	60	3.73					0.40				

[a] Obtained from the Arrhenius plot of the Henry (1) and Friedel-Crafts (2) reactions between 30 and 60 °C: $\ln k = lnA - \frac{E}{RT}$; R = 8.31 J/mol·K

[b] Obtained from the Eyring plot of the Henry (1) and Friedel-Crafts (2) reactions between 30 and 60 °C: $\ln\frac{k}{T} = ln\frac{k_B}{h} + \frac{\Delta S^{\neq}}{R} - \frac{\Delta H^{\neq}}{RT}$; k_B = $1.38\cdot10^{-23}$ J/K; h = $6.63\cdot10^{-34}$ J·s

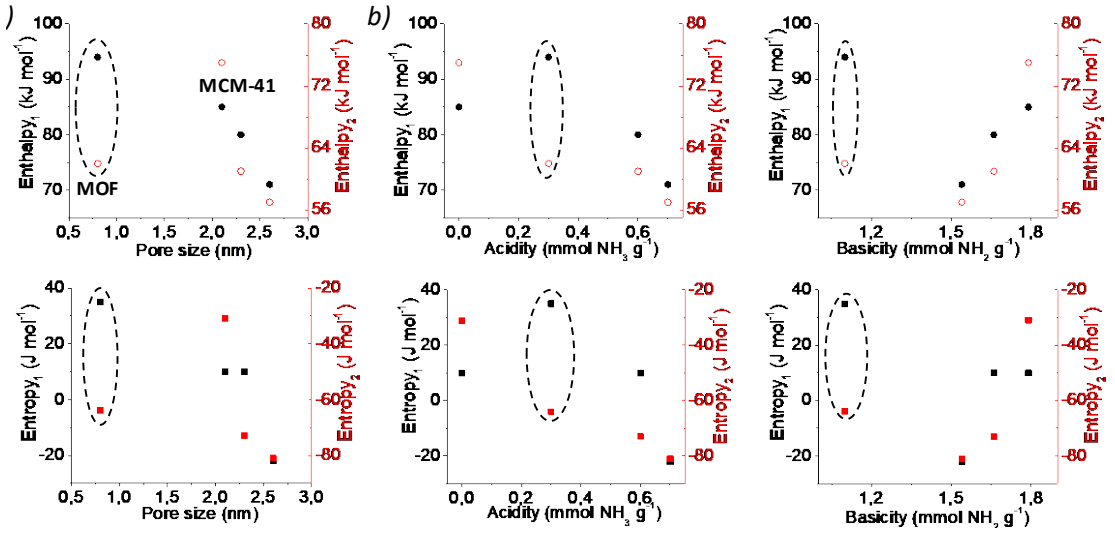

Figure S5. Kinetic dependence of physicochemical properties of the catalysts: pore size (a, d), acidity (b, e) and N content (basicity c, f). The values of $\Delta H^{\neq}$ (a-c) and $\Delta S^{\neq}$ (d-f) are obtained from the Eyring plot ($\ln\frac{k}{T} = ln\frac{k_B}{h} + \frac{\Delta S^{\neq}}{R} - \frac{\Delta H^{\neq}}{RT}$; k_B = $1.38\cdot10^{-23}$ J/K; h = $6.63\cdot10^{-34}$ J·s) of the Henry (1, black axis) and Friedel-Crafts (2, red axis) reactions between 30 and 60 °C.

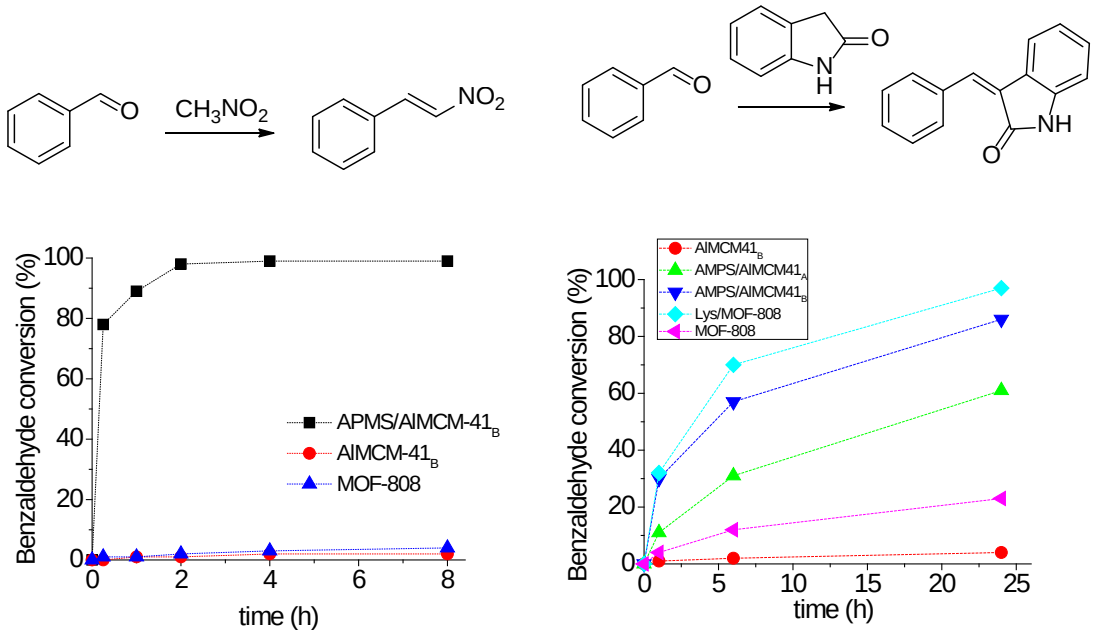

(a) (b)

Figure S6. Aldol condensation between benzaldehyde and nitromethane (a) or (b) oxindole using AlMCM-41 (Si/Al = 60) with and without amino groups.